DOI: 10.1002/ejoc.200600974

Ring–Chain Tautomerism of Simplified Analogues of Isoniazid–NAD(P) Adducts: an Experimental and Theoretical Study

Tamara Delaine,[a] Vania Bernardes-Génisson,[a] Jean-Luc Stigliani,[a] Heinz Gornitzka,[b] Bernard Meunier,[a][‡] and and Jean Bernadou*[a]

Keywords: Tautomerism / Hemiamidal / Computer chemistry / Isoniazid / Tuberculosis

Simplified analogues of oxidized and reduced isoniazid–NAD(P) adducts were prepared to study their behaviour with regard to ring–chain tautomeric isomerism in solution. In DMSO, the oxidized analogues (pyridinium salts) and the corresponding 1,2-dihydropyridine-reduced compounds were found to exist exclusively in the ring (cyclic hemiamidal) form. In contrast, the 1,4-dihydropyridine-reduced analogues were present in the ring and/or chain forms depending on the nature of the aromatic substituent. The 1,4-dihydropyridines (Ar = Ph, 3Cl-Py) are, in solution, preferentially in the keto–amide chain form, whereas the pyridine analogue (Ar = Py), which is the closest model of the isoniazid–NAD(P) adduct, exists as ring (major) and chain (minor) tautomers in equilibrium. The ratio of the tautomeric forms involved in the equilibrium of this system is also influenced by the polarity of the solvent with a shift towards the ring tautomer when the polarity of the solvent is increased. Complementary computational studies were performed by using quantum chemical calculations (B3LYP/6-31G**) and frontier molecular orbital analysis, which allowed the key structural factors involved in the ring–chain tautomerism equilibrium to be discussed.

Introduction

Tuberculosis (TB), the leading bacterial cause of infectious disease mortality, is observed with increasing incidence in both developing and industrialized countries. Drug-resistant strains of *Mycobacterium tuberculosis* (Mtb), in association with the deep synergy of TB with human immunodeficiency virus (HIV), are the major contributors. The emergence of antibiotic-resistant pathogen agents is a serious health problem worldwide today. Consequently, the importance of the design and development of drugs with new mechanisms of action, particularly as no new effective treatment has been introduced since 1971 after the approval of rifampicin,[1] is critical.

The old drug isoniazid (INH) exhibits high activity against Mtb and is still the drug most widely and efficiently used in antituberculous regimens.[2–4] However, bacterial strains resistant to INH are becoming current nowadays. Although INH is an old and simple molecule, its molecular mechanism of action is not completely elucidated. The consensus opinion is that a Mtb catalase–peroxidase (KatG) oxidizes INH, a prodrug, to an isonicotinoyl radical, which then couples covalently to the NAD(P) cofactors. The resulting INH–NAD(P) adducts [INH–NAD(P) is an abbreviation for adducts of isoniazid (INH) with either NAD or NADP cofactors] are potent inhibitors of InhA and MabA, two key reductases that are involved in Mtb cell wall biosynthesis[5–7] (Scheme 1). Recently, the Mtb dihydrofolate reductase, an enzyme essential for nucleic acid synthesis, has been proposed as an alternative target for the isoniazid–NADP adduct.[8]

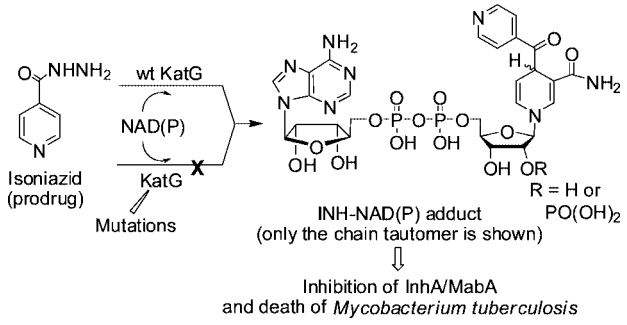

Scheme 1. Proposed mode of activation of the prodrug isoniazid and mechanism of action.

It has been reported that a substantial fraction of all clinical isolates which are resistant to INH results from KatG mutations.[9–10] Consequently, compounds that are inspired from INH–NAD(P) adducts structure and able to directly inhibit the ultimate molecular targets (InhA, MabA) of isoniazid, without requiring activation by KatG, have tremendous promise as novel drugs for combating multidrug-re-

[a] Laboratoire de Chimie de Coordination du CNRS,
205 route de Narbonne, 31077 Toulouse cedex 04, France
E-mail: bernadou@lcc-toulouse.fr
[b] Laboratoire d'Hétérochimie Fondamentale et Appliquée (UMR 5069), Université Paul Sabatier,
118 route de Narbonne, 31062 Toulouse cedex 04, France
[‡] Present address: Palumed, B. P. 28262, 31682 Labège cedex, France

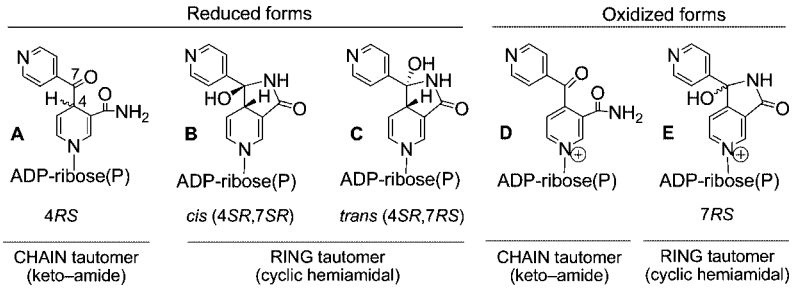

Figure 1. Proposed structures for reduced and oxidized forms of isoniazid–NAD(P) adducts.

sistant tuberculosis. Nevertheless, the exact chemical structure of the INH–NAD(P) adducts is not yet completely defined. Recent studies have suggested that INH–NAD(P) adducts exist as a structure with an isonicotinoyl radical bound at the C4 position of the nicotinamide residue in a chain (keto–amide) structure, forms **A** (reduced form) and **D** (oxidized form) (Figure 1).[8,11,12] Otherwise, we have shown without ambiguity that the oxidized pyridinium INH–NAD adduct exhibits cyclic hemiamidal structure **E**.[13] Moreover, we have also published that in solution the 1,4-dihydropyridine (reduced INH–NAD adducts) exists preferentially in ring form **C** (60%, *trans* cyclic hemiamidal) along with 40% of chain form **A** (keto–amide). An insignificant amount of ring form **B** (*cis* cyclic hemiamidal) could also be detected.[14] However, no experimental evidence reported so far supports the existence of an equilibrium between the two forms, ring and chain, in solution.

Our research project, based on the understanding of the mechanism of action of INH to develop new antitubercular agents, prompted us to deepen our investigation on the ring–chain tautomerism of INH adduct analogues with a γ-ketocarboxamide structure that could potentially cyclize in solution. This phenomenon is of primary interest as it can control the chemical and biological behaviour, for example solubility and lipophilicity, and the isoniazid analogue possesses the ability to strongly and selectively bind to the active site of the target enzyme(s). In this work, the ring–chain tautomerism was examined through both practical and theoretical experiments by using INH–NAD(P)-simplified analogues. A review on similar ring–chain tautomeric observations has been previously published.[15]

Results and Discussion

Experimental Study

The main objective of our previous work was the development of synthetic pathways for the preparation of hemiamidals **1** (Scheme 2).[16,17] Notably, despite the synthetic way, 4-aroylnicotinamides (i.e. the chain keto–amide tautomer) were never observed, and only cyclic hemiamidal **1** was formed. These starting compounds represent the precursors of pyridinium salts **2** and 1,4-dihydropyridines **3**, which can be useful simplified analogues of oxidized and reduced INH–NAD(P) adducts, respectively, for the ring–chain tautomerism study (Scheme 2).

The 1,4- (**3a′/3a′′** and **3b′/3b′′**) and 1,2-dihydropyridine (**4a** and **4b**) compounds were synthesized by reduction of the corresponding pyridinium salts **2** with the use of either $NaBH(OAc)_3$ or $NaBH_4$ (methods iii and ii, respectively,

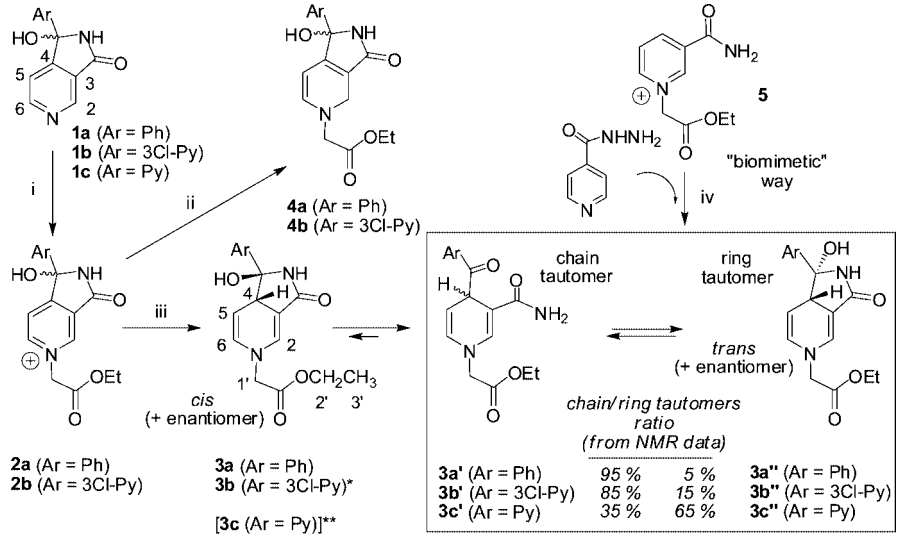

Scheme 2. Syntheses of the simplified analogues and conditions: (i) $BrCH_2COOEt$/THF; (ii) $NaBH_4$/EtOH; (iii) $NaBH(OAc)_3$ in AcOH/EtOH (1:5); (iv) $Mn(H_2P_2O_7)_3$, phosphate buffer pH 7.5. * Only detected in trace amounts by NMR spectroscopy. ** Only detected in trace amounts by NMR spectroscopy when **3c′/3c′′** were prepared by the biomimetic route.

Scheme 2). The regioselectivity and the stereoselectivity observed with $NaBH(OAc)_3$ can be explained by the assistance of the hemiamidal hydroxy group in this step. We propose that this hydroxy group interacts more easily with the boron atom of $NaBH(OAc)_3$ than with that in $NaBH_4$ to form an intermediate species able to transfer one hydride on the vicinal C4 position on the same side as the OH group. This hypothesis is indeed in agreement with the observed regioselectivity and stereochemistry of the reduction step. In the case of 1,4-dihydropyridines **3c′/3c′′**, they were prepared through a biomimetic approach[14,18] by using manganese(III) pyrophosphate as the stoichiometric oxidant as previously described (method iv, Scheme 2; 57% yield).[19] With these various compounds in hand, we studied their possibility to exist in solution in tautomeric ring and chain forms.

Starting compounds **1a**,[16,17] **1b** (this work) and **1c**[19] in a DMSO solution were exclusively found in a cyclic hemiamidal form as shown by ^{1}H NMR [δ(NH) = 9.48–9.65 ppm, δ(OH) = 7.18–7.65 ppm] and ^{13}C NMR (tetrahedral C7 at δ = 84.7–88.1 ppm) spectroscopic analysis. No chain (keto–amide) isomer could be detected by NMR spectroscopy. Furthermore, the data of the X-ray crystalline structure analyses of **1a**[16] and **1b** (Figure 2) also confirmed the cyclized framework.

The same behaviour was also observed for pyridinium salts **2a** and **2b** and for 1,2-dihydropyridines **4a** and **4b** as verified by ^{13}C NMR spectroscopic analysis (C7 detected as a tetrahedron carbon in the range 84 to 90 ppm). Concerning the pyridinium salts, this result is in agreement with our previous work in which we demonstrated that the oxidized INH–NAD adduct only exists in a cyclized form.[13] Altogether, these results indicate that the preference for the ring tautomeric form of **1**, **2** and **4** is probably associated with the sp^2 hybridization of the C3 and C4 atoms, which are the α and β carbons with respect to the amide group, respectively. Indeed, for all studied compounds with sp^2 hybridization at the α and β carbons, the ring form was exclusive.

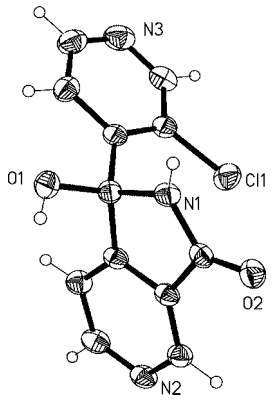

Figure 2. X-ray structure of compound **1b**.

In contrast, the regio and stereoselective reduction of cyclized pyridinium salt **2a** (Ar = Ph) with $NaBH(OAc)_3$ initially gave the 1,4-dihydropyridine of *cis* hemiamidal **3a** (4-

Table 1. ^{1}H NMR chemical shifts [ppm] and coupling constants [Hz] for **3a**, **3b**, **3c**,[a] **3a′**, **3b′**, **3c′**, **3a′′**, **3b′′**, **3c′′**, **4a** and **4b** in DMSO solution. See Scheme 2 for numbering of H atoms.

Tautomers		2-H	4-H	5-H	6-H	H aromatic	1′-H, 2′-H	3′-H
3a	*cis* ring	6.70, s	3.79, d *J* = 1.5	3.91, dd *J* = 7.8, 1.5	5.67, d *J* = 7.8	7.31–7.25 (5 H)	4.08, s + q	1.17
3a′	chain	7.21, d *J* = 1.2	5.05, dd *J* = 4.6, 1.2	4.64, dd *J* = 7.8, 4.6	6.05, d *J* = 7.8, 1.2	8.00–7.50 (5 H)	4.12, s + q	1.20
3a′′	*trans* ring	6.79, s	3.50, d *J* = 1.8	4.45, dd *J* = 7.5, 1.8	6.00, d *J* ND	7.63–7.20 (5 H)	4.15	1.20
3b	*cis* ring	6.75, s	3.81, dd *J* = 1.8, 1.8	masked	5.80, dd *J* = 8.0, 1.5	8.7–8.4 (2 H) 7.9–7.8 (1 H)	4.3–4.1, m	1.20
3b′	chain	7.20, d *J* = 1.0	4.70, dd *J* = 4.7, 0.8	4.62, dd *J* = 7.7, 4.6	6.17, d *J* = 7.8	8.71, s (1 H) 8.62, d, *J* = 5.0 (1 H) 7.79, d, *J* = 4.6 (1 H)	4.3–4.1, m	1.20
3b′′	*trans* ring	6.80, d *J* = 2.0	masked	4.45, dd *J* = 7.6, 1.4	6.05, ddd *J* = 7.5, ND	8.7–8.4 (2 H) 7.9–7.8 (1 H)	4.3–4.1, m	1.20
3c	*cis* ring	6.74, s	3.83, d *J* = 1.0	3.93, dd *J* = 7.8, 1.0	5.72, d *J* = 7.7	8.84 (2 H) 7.27 (2 H)	4.3–4.1, m	1.20
3c′	chain	7.21, d *J* = 1.1	4.97, dd *J* = 4.5, 1.0	4.64, dd *J* = 7.8, 4.5	6.11, d *J* = 7.8	8.78, br. s (2 H) 7.86, d, *J* = 5.9 (2 H)	4.15, m	1.19
3c′′	*trans* ring	6.83, s	3.53, d *J* = 1.6	4.51, dd *J* = 7.6, 1.5	6.04, d *J* = 7.8	8.54, br. s (2 H) 7.50, d, *J* = 4.1 (2 H)	4.15, m	1.19
4a	ring	3.88, s 3.91, s	–	4.45, d *J* = 7.2	6.39, d *J* = 6.9	7.30, m (5 H)	4.22, s 4.13, q, *J* = 7.1	1.21, t *J* = 7.1
4b	ring	3.92, s 3.94, s	–	4.27, d *J* = 6.8	6.41, d *J* = 7.0	8.55, d, *J* = 6.7 (1 H) 8.53, s (1 H) 7.86, d, *J* = 5.1 (1 H)	4.26, s 4.11, q, *J* = 6.8	1.21, t *J* = 7.1

[a] Very low amount of **3c** was detected by ^{1}H NMR spectroscopic analysis during the preparation of **3c′/3c′′** (method iv, Scheme 2). ND = not determined.

H at 3.82 ppm), which spontaneously opened to give chain isomer **3a′** (4-H at δ = 5.05 ppm) as the main compound (95%) (Table 1), whereas *trans* hemiamidal **3a′′** was only detected in trace amounts (5%). The reduction of **2b** (Ar = 3Cl-Py) with $NaBH(OAc)_3$ mainly gave (85%) dihydropyridine chain form **3b′** along with 15% of *trans* cyclic hemiamidal **3b′′**. The *cis* cyclic hemiamidal **3b** initially formed after the reduction step was only detected in low amounts, which suggests that the isomerization of **3b** towards **3b′** proceeds very quickly. In the series Ar = Py, 1,4-dihydropyridines could not be prepared by following methods i/iii because selective alkylation of **1c** at the nitrogen atom of the nicotinamide moiety could not be achieved.[19] Therefore, this series of 1,4-dihydropyridines was obtained by following the biomimetic strategy by oxidation of isoniazid with manganese(III) pyrophosphate in the presence of pyridinium salt **5** (method iv, Scheme 2). These 1,4-dihydropyridines exist in chain and *trans* ring forms **3c′** and **3c′′**, respectively. The NMR spectrum of the mixture of adducts exhibited two major sets of signals with 4-H at δ = 3.53 ppm and at δ = 4.97 ppm (Table 1), which indicates that the adducts exist in the *trans* cyclic hemiamidal form in 65% and in the keto–amide chain form in 35%. These results are also in line with previous NMR spectroscopic data obtained by our group for INH–NAD adducts, which suggests a ring/chain ratio of 60:40.

By ^1H NMR spectroscopic analysis (DMSO, room temperature) we could identify and quantify the unstable chain and ring tautomers of 1,4-dihydropyridines in solution (Table 1). The 4-H resonances of the *trans* ring form (4*SR*,7*RS*) at 3.5 ppm, and of the chain form (4*SR*) at 5.1 ppm, represent the most selective and convenient signal to discriminate between these two tautomeric isomers. Attribution of the 4-H resonances was extrapolated from the chain and ring INH–NAD adduct, previously characterized in our group.[20]

Because cyclized compounds were observed as the major tautomers only for pyridine analogue **3** (Ar = Py) when prepared by the biomimetic approach, we wondered if manganese(III) pyrophosphate could facilitate the cyclization process or, alternatively, if the difference in the observed behaviour of molecules **3a′**, **3b′** and **3c′** could be attributed to the nature of the aromatic substituent (Ar = Ph, 3Cl-Py and Py, respectively). In this context, we tried to obtain **3a′** (Ar = Ph), which was found to exist in a chain structure, by the biomimetic approach by using benzoylhydrazine, manganese(III) pyrophosphate and pyridinium salt **5**. Unfortunately, 1,4-dihydropyridines could not be formed in this manner. The oxidation of the hydrazide of benzoic acid by manganese pyrophosphate directly and exclusively led to benzoic acid. Otherwise, when keto–amide compound **3a′** (Scheme 2, method i/iii) was incubated under the same conditions as for the biomimetic reaction (Scheme 2, method iv) no evolution of the chain form could be observed, which rules out the hypothesis of an eventual cyclization process promoted by the biomimetic conditions.

At this stage, we also wondered if the ring–chain tautomerism might exist in dynamic equilibrium. In this way, by HPLC we collected the major **3c′′** peak and the minor **3c′** peak from the purified biomimetic reaction mixture; we could check that subsequent separated reinjection of these samples provided in both cases the same chromatographic profile as the initial one, which suggests that a dynamic equilibrium occurs between these two main compounds. The equilibrium **3c′**/**3c′′** could also be evidenced by the solvent effect on the ratio of the ring/chain forms: determined from the ratio of the 4-H signal areas in the $CDCl_3$ and DMSO NMR spectra, the ratio of ring/chain tautomers was around 65:35 and it increases to 85:15 in DMSO/H_2O (1:1). When the medium polarity is increased, the tautomeric equilibrium shifts towards the cyclized structure.

Altogether these results indicate that, aside from the sp^2 hybridization of the C3/C4 carbon atoms, the nature of the aromatic substituent as well as the polarity of the medium have an important influence upon the ring–chain tautomerism process. As an extension of our experimental work, we thought that supplementary computational methods could also be useful in the determination of the relative stability of the ring–chain tautomers by calculating tautomerization energies.

Computational Study

In order to decrease the computational constraint (time consuming), we decided to adopt a simplified model where the $CH_2COOC_2H_5$ residue of structure **3** was replaced by a CH_3 group (Scheme 3). The chain tautomeric structure of **6** can exist in different conformations depending on the relative orientation of the ketone carbonyl group. For this reason, a conformational analysis was carried out by varying the rotation angle of the H–C4–C7–O bond with the use of the AM1 Hamiltonian method. Two energetically favourable conformations were found (Figure 3): a folded conformation for which the aromatic group is oriented over the dihydropyridine ring (conformation I, dihedral angles H–C4–C7–O calculated by B3LYP/6-31G** 16°, 29° and 18° for compounds **6a′**, **6b′**, and **6c′**, respectively) and an extended conformation where these groups are oriented away from each other (conformation II, dihedral angles H–C4–C7–O of 134°, 111° and 133° for compounds **6a′**, **6b′**, and **6c′**, respectively). For each chain tautomer, we therefore studied both conformations.

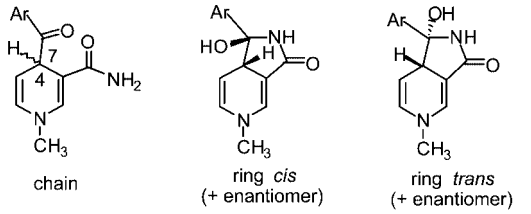

6a' (Ar = Ph) **6a** (Ar = Ph) **6a''** (Ar = Ph)
6b' (Ar = 3Cl-Py) **6b** (Ar = 3Cl-Py) **6b''** (Ar = 3Cl-Py)
6c' (Ar = Py) **6c** (Ar = Py) **6c''** (Ar = Py)

Scheme 3. Simplified analogues for computational study.

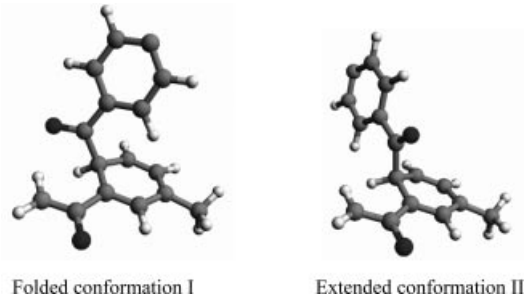

Figure 3. The two most energetically favoured conformations of keto–amide models **6** (the case of **6c′** is shown).

Relative free enthalpies of the optimized geometries (B3LYP/6-31G**) of compounds **6** in the gas phase as well as in DMSO are listed in Table 2. In the gas phase, folded chain compounds **6a′**, **6b′** and **6c′** are predicted to be more stable than both the chain extended structures and the two *cis* and *trans* ring forms. Between the two cyclized forms, the *cis* form is in all cases the least stable. The free Gibbs energy difference between the *trans* ring and the folded chain tautomers ($\Delta G° = G°_{trans\ ring} - G°_{folded\ chain}$) was 4.51 kcal mol^{-1} for benzoyl **6a′** and 4.12 kcal mol^{-1} for the *m*-chloroisonicotinoyl **6b′** derivative. These differences in energies indicate that these compounds have no tendency to cyclize as was experimentally observed. For isonicotinoyl analogue **6c′**, which is presumed to mainly exist in cyclic form **6c′′** (by reference to experimental data for analogue **3c′**), the energy difference is lowered, but it remains positive (2.77 kcal mol^{-1}) and does not explain the preference for the ring structure.

It is interesting to note that inclusion of bulk solvent effects by the polarized continuum model of solvation (DMSO) leads to a decrease in the free energies of about 15–20 kcal mol^{-1} depending on the derivatives. The solvent acts by stabilizing the extended conformations, which are the preferred forms. The relative stabilization of the extended forms in DMSO can be explained by their higher accessible surface for the polar solvation medium. The energy difference between the *trans* ring and the chain forms is less marked for benzoyl **6a′** (3.78 kcal mol^{-1}) and *m*-chloroisonicotinoyl **6b′** (1.57 kcal mol^{-1}) than in the vacuum medium. On the basis of these differences in energies, the predicted abundances of each tautomer was theoretically determined by using the Boltzmann equation at a temperature of 298 K. The calculated population of the chain form (more stable) of **6a′** and **6b′** for these two compounds was found to be 99.8 and 93%, respectively. These values are in accord with our experimental results collected in Table 2. However, the calculated difference in energy found for pyridine analogues **6c′′**/**6c′** ($G°$**6c′′** – $G°$**6c′** = 2.91 kcal mol^{-1}) does not reflect the experimental data. In fact, the equilibrium constant K_E = ring/chain = 1.86 calculated from NMR spectroscopic data for **3c′′**/**3c′** would be associated to a difference in energy between these two forms of about –0.24 kcal mol^{-1}.

This solvation model probably does not take into account some direct interactions between the solvent molecules and a part of the compounds framework (i.e. the amide group). Thereby, to complete this thermodynamic approach, we focused our attention on a frontier molecular orbital analysis. The cyclization process can indeed be described as a nucleophilic attack of the amide nitrogen atom at the carbonyl carbon atom followed by transfer of the amide hydrogen towards the oxygen atom. This process could be accomplished if large highest occupied molecular orbital (HOMO) coefficients are found on the nitrogen atom and if the large lowest unoccupied molecular orbital (LUMO) coefficients are well-characterized at the carbonyl carbon atom. The lower the energy difference between these two orbitals (LUMO – HOMO) the greater the propensity to form the cyclic form. Molecular orbital calculations performed at the B3LYP/6-31G** level of theory show that the LUMO effectively displays large atomic orbital coefficients on the carbonyl carbon. The HOMO does not display significant coefficients either at the nitrogen or the oxygen atom. However, these coefficients are more expanded on the

Table 2. Relative free enthalpies[a] [kcal mol^{-1}] of compounds **6** calculated (B3LYP/6-31G**) in the gas phase and in DMSO[b] with percent population and frontier orbital energy differences.

	Ar	Tautomer forms[c]	$\Delta G°$ (gas phase)	$\Delta G°$ (DMSO)	Boltzmann ratio[d]	Population by NMR[e]	LUMO – HOMO[b,f]	LUMO – HOMO$_{-1}$[b,f]	LUMO – HOMO$_{-2}$[b,f]
6a′	Ph	chain	0.00[g]	0.00[h]	99.8	95	3.40	4.92	5.10
6a		*cis* ring	8.01	5.05	–	–	–	–	–
6a′′		*trans* ring	4.51	3.78	0.2	5	–	–	–
6b′	3Cl-Py	chain	0.00[g]	0.00[h]	93	85	3.34	4.77	5.06
6b		*cis* ring	7.54	3.57	–	–	–	–	–
6b′′		*trans* ring	4.12	1.57	7	15	–	–	–
6c′	Py	chain	0.00[g]	0.00[h]	99	35	3.22	4.70	4.84
6c		*cis* ring	5.55	4.53	–	–	–	–	–
6c′′		*trans* ring	2.77	2.91	1	65	–	–	–

[a] The free enthalpy of the most stable tautomer for each entry is taken as reference. [b] Calculated with the polarizable continuum model (PCM). [c] See Scheme 3 for structures. [d] Calculated according to the Boltzmann equation at T = 298 K. [e] By reference to data for analogues **3a′**/**3a′′**, **3b′**/**3b′′**, **3c′**/**3c′′**. [f] Energy difference between the LUMO and the first three HOMOs [eV]. [g] Folded conformation. [h] Extended conformation (see Figure 3).

second and mostly on the third occupied molecular orbitals. Moreover, these later HOMO orbitals are on very close energy levels (the energy difference varies between 0.1 and 0.3 eV). The energy differences between the LUMO and the three first HOMOs of the tautomers are displayed in Table 2. One can notice, as a general rule, that the higher energy separations are found for chain derivatives **6a′** and **6b′**, whereas tighter gaps are found for isonicotinoyl analogue **6c′**, which suggests that the latter has more propensity for an intramolecular cyclization. This was indeed the behaviour observed in practice for the corresponding derivatives **3a′**, **3b′** and **3c′**: the ratio of chain/ring tautomers determined from NMR spectroscopic data decreases in the order **3a′** > **3b′** > **3c′** (Table 2).

In summary, we have prepared and studied some simplified oxidized and reduced models of INH–NAD(P) adducts with regard to ring–chain tautomerism. It was shown in solution that ring–chain tautomerism is not observed for the 1,2-dihydropyridines and pyridinium analogues which have sp^2 hybridization at the α and β carbon (C3 and C4 of the nicotinamide ring). In contrast, this phenomenon occurs in the 1,4 dihydropyridine series to give rise to both chain and ring forms. Experimental evidence as well as theoretical data have shown that the preferred tautomeric form in solution is highly dependent on the nature of the aromatic substituent and on the medium. For pyridine analogues **3c′/3c′′**, the closest model of the INH–NAD(P) adducts, the preferential form in both media (apolar and polar) is the ring tautomer. Because the most recent results on the inhibition of molecular targets of INH show that INH–NAD(P) adducts in a chain form are involved, it might be concluded that the design of simplified analogues of these biologically relevant species should either favour compounds with a chain structure or consider derivatives in a cyclized form as prodrugs that are able to release the bioactive chain molecule in vivo through ring–chain tautomeric equilibrium.

Experimental Section

HPLC analyses were performed on a reverse phase column (PS DVB, 5 μm, 250 × 4.6 mm) by using a linear gradient from 100% CH_3COONH_4 (70 mM, pH 7) aqueous solution to 50% acetonitrile during 60 min for analyses of the **3c′/3c′′** mixture (flow rate 1 mL/min). The column was coupled to a UV detector (Kontron) for detection at 330 nm. Calculations were performed with the use of the Gaussian 03 program suite.[21] Starting geometries were initially obtained through a conformational search at the AM1 level.[22] The most stable geometries were completely optimized at the B3LYP/6-31G** level of theory[23] by utilizing the gradient technique and default thresholds for convergence. Each stationary point was characterized by frequency calculation (no negative imaginary frequency for a minimum). Thermodynamic data were calculated at 298 K and 1 atm. Zero-point energies were unscaled. The solvent effect was taken into account by including electrostatic solvent interactions. The bulk solvent effect was estimated with the polarizable continuum model (PCM),[24,25] with DMSO as the solvent (ε = 46.7). Compounds **1a**, **2a**, **3a**, **3a′/3a′′** and **4a**,[17] **1c**, **3c′/3c′′** and **5**[19] were prepared as previously reported.

1-(3-Chloropyridin-4-yl)-1-hydroxy-1,2-dihydro-3*H*-pyrrolo[3,4-*c*]pyridin-3-one (1b): A solution of 3,4-pyridinedicarboximide (2.0 g, 13.5 mmol) and 3-chloropyridine (2.84 mL, 29.6 mmol) in dry THF (100 mL), under an argon atmosphere cooled to –95 °C, was treated dropwise with lithium diisopropylamide (16.5 mL, 2.0 M in THF/*n*-heptane, 33.0 mmol), and the mixture was stirred at –80 °C for 1 h and then warmed to room temperature over 4 h. Water was added, and the solvent was evaporated under vacuum. The crude product was purified by silica gel column chromatography (CH_2Cl_2/MeOH 100:0 to 80:20). The yellow solid was recrystallized from acetone to give hemiamidal **1b** as a white solid (542 mg, 15%). M.p.: 226–227 °C. IR (KBr): $\tilde{\nu}$ = 3285, 3171, 3043, 2811, 1701, 1613 cm^{-1}. ^1H NMR (250 MHz, [D$_6$]DMSO): δ = 9.48 (br. s, 1 H), 8.92 (d, J = 0.9 Hz, 1 H), 8.76 (d, J = 4.9 Hz, 1 H), 8.67 (d, J = 5.1 Hz, 1 H), 8.51 (s, 1 H), 8.13 (d, J = 5.1 Hz, 1 H), 7.65 (br. s, 1 H), 7.31 (dd, J = 1.2 Hz and 5.0 Hz, 1 H) ppm. ^{13}C NMR (63 MHz, [D$_6$]DMSO): δ = 167.7 (C$_q$), 155.9 (C$_q$), 153.2 (CH), 150.3 (CH), 148.5 (CH), 145.0 (C$_q$), 144.4 (CH), 128.5 (C$_q$), 127.9 (C$_q$), 123.6 (CH), 117.4 (CH), 84.7 (C$_q$) ppm. MS (ESI+): m/z = 545 [2M + Na]$^+$, 284 [M + Na]$^+$, 262 [M + H]$^+$. HRMS (ESI): calcd. for $C_{12}H_9ClN_3O_2$ 262.0383; found 262.0385. Crystal Data for Compound **1b**: $C_{12}H_8ClN_3O_2$, M = 261.66, triclinic, $P\bar{1}$, a = 7.556(1) Å, b = 8.254(1) Å, c = 10.445(1) Å, α = 75.142(2)°, β = 72.994(2)°, γ = 63.030(2)°, V = 549.31(10) Å^3, Z = 2, T = 173(2) K, 3251 reflections (2225 independent, R_{int} = 0.0125) were collected. Largest electron density residue: 0.335 e Å^{-3}, R_1 [for $I > 2\sigma(I)$] = 0.0314 and wR_2 = 0.0865 (all data) with $R_1 = \Sigma||F_o| - |F_c||/\Sigma|F_o|$ and $wR_2 = [\Sigma w (F_o^2 - F_c^2)^2/\Sigma w(F_o^2)^2]^{0.5}$. All data for the structure represented in this paper were collected at low temperature by using an oil-coated shock-cooled crystal with a Bruker AXS CCD 1000 diffractometer and with Mo-K_α radiation (λ = 0.71073 Å). The structure was solved by direct methods[26] and all non-hydrogen atoms were refined anisotropically by using the least-squares method on F^2.[27] CCDC-621385 contains the supplementary crystallographic data for this paper. These data can be obtained free of charge from The Cambridge Crystallographic Data Centre via www.ccdc.cam.ac.uk/data_request/cif.

1-(3-Chloropyridin-4-yl)-5-[2-(ethyloxy)-2-oxoethyl]-1-hydroxy-3-oxo-1,2-dihydro-3*H*-pyrrolo[3,4-*c*]pyridinium Trifluoroacetate (2b): A solution of hemiamidal **1b** (300 mg, 1.14 mmol) heated at reflux in dry THF (50 mL), under an argon atmosphere was treated dropwise with ethyl bromoacetate (380 mg, 2.28 mmol). After 48 h, ether (40 mL) was added, and the purple precipitate was filtered, washed with dichloromethane, acetone and ether and dried under vacuum. The purple powder was purified by semi-preparative HPLC (0.1% TFA/MeOH 90:10 to 50:50) to give **2b** (counterion CF_3COO^-) (162 mg, 33%). IR (KBr): $\tilde{\nu}$ = 3424, 3062, 2853,1736, 1676 cm^{-1}. ^1H NMR (250 MHz, [D$_6$]DMSO): δ = 10.28 (s, 1 H), 9.64 (s, 1 H), 9.26 (d, J = 6.1 Hz, 1 H), 8.76 (br. s, 1 H), 8.61 (s, 1 H), 8.28 (d, J = 6.2 Hz, 1 H), 8.19 (d, J = 4.6 Hz, 1 H), 5.74 (s, 2 H), 4.25 (q, J = 7.1 Hz, 2 H), 1.26 (t, J = 7.1 Hz, 3 H) ppm. ^{13}C NMR (63 MHz, [D$_6$]DMSO): δ = 167.3 (C$_q$, CF_3COO), 166.1 (C$_q$) 163.6 (C$_q$), 158.3 (C$_q$, CF_3COO), 150.9 (CH), 150.3 (CH), 148.9 (CH), 142.8 (C$_q$), 142.7 (CH), 131.4 (C$_q$), 128.3 (C$_q$), 123.7 (CH) 121.4 (CH), 85.0 (C$_q$), 62.3 (CH_2), 60.7 (CH_2), 13.8 (CH_3), (1 C$_q$ missing) ppm. MS (FAB, MNBA): m/z = 348 [M]$^+$, 334 [M – CH_2]$^+$, 320 [M – CH_2CH_2]$^+$. HRMS (FAB): calcd. for $C_{16}H_{15}ClN_3O_4$ 348.0751; found 348.0750.

Mixture of Ethyl [4-(3-Chloro-4-isonicotinoyl)-3-aminocarbonyl-1,4-dihydropyridin-1-yl]acetate (3b′) and Ethyl [1-Hydroxy-3-oxo-1-(3-chloropyridin-4-yl)-1,2,5,7a-tetrahydro-3*H*-pyrrolo[3,4-*c*]pyridin-5-yl]acetate (3b′′): A solution of **2b** (80 mg, 0.19 mmol) in ethanol (7.6 mL) at –10 °C, under an argon atmosphere was treated with a

solution of sodium triacetoxyborohydride (67 mg, 0.32 mmol) in acetic acid (1.6 mL). After 5 min at –10 °C, water was added, and the product was extracted with ethyl acetate. The combined organic phase was washed with saturated $NaHCO_3$ solution, dried with Na_2SO_4 and concentrated in vacuo to give an unstable mixture of tautomers **3b′/3b′′** as a yellow oil (27 mg, 42%). For ^1H NMR spectroscopic data see Table 1. MS (FAB): *m/z* = 316 $[M]^+$, 314 $[M - 2]^+$.

Ethyl (1-Hydroxy-3-oxo-1-(3-chloropyridin-4-yl)-1,2,4,5-tetrahydro-3*H*-pyrrolo[3,4-*c*]pyridin-5-yl)acetate (4b): A solution of **2b** (80 mg, 0,19 mmol) in ethanol (7.2 mL) at 0 °C, under an argon atmosphere, was treated with sodium borohydride (8.2 mg, 0,22 mmol). After 10 min at 0 °C, water was added, and the product was extracted with ethyl acetate. The organic phase was dried with Na_2SO_4, and the solvent was evaporated under vacuum. The crude product was purified by silica gel chromatography (dichloromethane/EtOH 100:0 to 80:20) to give **4b** as a yellow oil (20 mg, 31%). IR: $\tilde{\nu}$ = 3331 (br.), 2920, 2850, 1728, 1678, 1650, 1552, 1191, 1104, 1030 cm^{-1}. ^1H NMR (250 MHz, [D$_6$]DMSO): δ = 8.55 (d, *J* = 6.7 Hz, 1 H), 8.53 (s, 1 H), 8.23 (s, 1 H, NH), 7.86 (d, *J* = 5.1 Hz, 1 H), 6.85 (s, 1 H, OH), 6.41 (d, *J* = 7.0 Hz, 1 H), 4.27 (d, *J* = 6.8 Hz, 1 H), 4.26 (s, 2 H), 4.11 (q, *J* = 6.8 Hz, 2 H), 3.92 and 3.94 (2 s, 2 H), 1.21 (t, *J* = 7.1 Hz, 3 H) ppm. ^{13}C NMR ([D$_6$]DMSO): δ = 176.5 and 174.5 (2 C_q), 158.0, 151.0, 128.7 and 117.5 (4 C_q), 155.5, 153.3 and 150.4 (3 CH_{ar}), 134.0 (CH), 91.3 (CH), 89.8 (C_q), 65.8, 60.2 and 50.8 (3 CH_2), 19.3 (CH_3) ppm. MS (DCI/NH_3): *m/z* = 348 $[M]^+$, 367 $[M + NH_4]^+$.

Acknowledgments

The authors would like to thank CALMIP (calcul intensif en Midi-Pyrenees, Toulouse, France) for computing facilities.

[1] W. Wehrli, *Top. Curr. Chem.* **1977**, *72*, 21–49.
[2] B. R. K. Bloom, C. J. Murray, *Science* **1992**, *257*, 1055–1064.
[3] K. Bartmann, H. Iwainski, H. H. Kleeberg, P. Mison, H. H. Offe, H. Otten, D. Tettenborn, L. Trnka in *Antituberculosis Drugs* (Ed.: K. Bartmann), Springer, Berlin, **1988**.
[4] J. S. Blanchard, *Annu. Rev. Biochem.* **1996**, *65*, 215–239.
[5] A. Quémard, C. Lacave, G. Lanéelle, *Antimicrob. Agents, Chemother.* **1991**, *35*, 1035–1039.
[6] A. Dessen, A. Quémard, J. S. Blanchard, W. R. Jacobs Jr, J. C. Sacchettini, *Science* **1995**, *267*, 1638–1641.
[7] S. Ducasse-Cabanot, M. Cohen-Gonsaud, H. Marrakchi, M. Nguyen, D. Zerbib, J. Bernadou, M. Daffé, G. Labesse, A. Quémard, *Antimicrob. Agents, Chemother.* **2004**, *48*, 242–249.
[8] A. Argyrou, M. W. Vetting, B. Aladegbami, J. S. Blanchard, *Nat. Struct. Mol. Biol.* **2006**, *13*, 408–413.
[9] B. Heym, N. Honoré, C. Truffot-Pernot, A. Banerjee, C. Schurra, W. R. Jacobs Jr, J. D. van Embden, J. H. Grosset, S. T. Cole, *Lancet* **1994**, *344*, 293–298.
[10] S. V. Ramaswamy, R. Reich, S. J. Dou, L. Jasperse, X. Pan, A. Wanger, T. Quituga, E. A. Graviss, *Antimicrob. Agents Chemother.* **2003**, *47*, 1241–1250.
[11] D. A. Rozwarski, G. A. Grant, D. H. R. Barton, W. R. Jacobs Jr, J. C. Sacchettini, *Science* **1998**, *279*, 98–102.
[12] M. Wilming, K. Johnsson, *Angew. Chem. Int. Ed.* **1999**, *38*, 2588–2590.
[13] S. Broussy, V. Bernardes-Génisson, Y. Coppel, A. Quémard, J. Bernadou, B. Meunier, *Org. Biomol. Chem.* **2005**, *3*, 670–673.
[14] M. Nguyen, C. Claparols, J. Bernadou, B. Meunier, *ChemBioChem* **2001**, *2*, 877–883.
[15] R. E. Valters, F. Fülöp, D. Korbonits in *Advances in Heterocyclic Chemistry, Vol. 64* (Ed.: A. Katritzky), Academic Press, **1995**, pp. 251–321; R. E. Valters, F. Fülöp, D. Korbonits in *Advances in Heterocyclic Chemistry, Vol. 66* (Ed.: A. Katritzky), Academic Press, **1996**, pp. 1–71.
[16] S. Broussy, V. Bernardes-Génisson, H. Gornitzka, J. Bernadou, B. Meunier, *Org. Biomol. Chem.* **2005**, *3*, 666–669.
[17] S. Broussy, V. Bernardes-Génisson, A. Quémard, B. Meunier, J. Bernadou, *J. Org. Chem.* **2005**, *70*, 10502–10510.
[18] M. Nguyen, A. Quémard, S. Broussy, J. Bernadou, B. Meunier, *Antimicrob. Agents Chemother.* **2002**, *46*, 2137–2144.
[19] T. Delaine, V. Bernardes-Génisson, B. Meunier, J. Bernadou, *J. Org. Chem.* **2007**, *72*, 675–678.
[20] S. Broussy, Y. Coppel, M. Nguyen, J. Bernadou, B. Meunier, *Chem. Eur. J.* **2003**, *9*, 2034–2038.
[21] M. J. Frisch, G. W. Trucks, H. B. Schlegel, G. E. Scuseria, M. A. Robb, J. R. Cheeseman, J. A. Montgomery Jr, T. Vreven, K. N. Kudin, J. C. Burant, J. M. Millam, S. S. Iyengar, J. Tomasi, V. Barone, B. Mennucci, M. Cossi, G. Scalmani, N. Rega, G. A. Petersson, H. Nakatsuji, M. Hada, M. Ehara, K. Toyota, R. Fukuda, J. Hasegawa, M. Ishida, T. Nakajima, Y. Honda, O. Kitao, H. Nakai, M. Klene, X. Li, J. E. Knox, H. P. Hratchian, J. B. Cross, C. Adamo, J. Jaramillo, R. Gomperts, R. E. Stratmann, O. Yazyev, A. J. Austin, R. Cammi, C. Pomelli, J. W. Ochterski, P. Y. Ayala, K. Morokuma, G. A. Voth, P. Salvador, J. J. Dannenberg, V. G. Zakrzewski, S. Dapprich, A. D. Daniels, M. C. Strain, O. Farkas, D. K. Malick, A. D. Rabuck, K. Raghavachari, J. B. Foresman, J. V. Ortiz, Q. Cui, A. G. Baboul, S. Clifford, J. Cioslowski, B. B. Stefanov, G. Liu, A. Liashenko, P. Piskorz, I. Komaromi, R. L. Martin, D. J. Fox, T. Keith, M. A. Al-Laham, C. Y. Peng, A. Nanayakkara, M. Challacombe, P. M. W. Gill, B. Johnson, W. Chen, M. W. Wong, C. Gonzalez, and J. A. Pople, *Gaussian 03*, Revision B.05, Gaussian, Inc., Pittsburgh, **2003**.
[22] M. J. S. Dewar, E. G. Zoebisch, E. F. Healy, J. J. P. Stewart, *J. Am. Chem. Soc.* **1985**, *107*, 3902–3909.
[23] A. D. Becke, *J. Chem. Phys.* **1993**, *98*, 5648–5652.
[24] R. Cammi, B. Mennucci, J. Tomasi, *J. Phys. Chem. A* **2000**, *104*, 5631–5637.
[25] M. Cossi, G. Scalmani, N. Rega, V. Barone, *J. Chem. Phys.* **2002**, *117*, 43–54.
[26] G. M. Sheldrick, SHELXS-97, *Acta Crystallogr., Sect. A* **1990**, *46*, 467–473.
[27] G. M. Sheldrick, *SHELXL-97: Program for Crystal Structure Refinement*, University of Göttingen, Göttingen, **1997**.

Received: November 7, 2006
Published Online: February 9, 2007

